PROCEEDINGS of the
23rd International Congress on Acoustics

9 to 13 September 2019 in Aachen, Germany

Comparisons of Two Virtual Sensing Methods for Broadband Noise

Reo MAEDA(1), Yoshinobu KAJIKAWA(2)

(1)Kansai University, Japan, leo0756.kansai@gmail.com

(2)Kansai University, Japan, kaji@kansai-u.ac.jp

Abstract

Conventional ANC systems can reduce a target noise around the error microphone. Hence, the users for ANC systems may not get sufficient noise reduction if the user's ears are apart from the error microphones. This is because the size of the Zone of Quite (ZoQ) is 1/10 of wavelength of the target noise. To solve this issue, some virtual sensing techniques have been already proposed and examined. These techniques can create the maximum noise reduction at the desired positions. In this paper, we introduce two methods, which are called "Remote Microphone" and "Auxiliary Filter based Virtual Sensing" methods to an ANC headrest in order to examine the effectiveness. In various situations, we implement the two virtual sensing techniques on the ANC headrest and compare the results through some simulations in MATLAB

Keywords: Active Noise Control, Virtual sensing technique, Remote Microphone method, Auxiliary Filter based Virtual Sensing method, Headrest

1 INTRODUCTION

Active Noise Control (ANC) is a means of reducing the unwanted noise. ANC is a technique based on the principle of superposition, i.e., an antinoise with the same amplitude and opposite phase is generated and combined with an unwanted noise, thus resulting in the cancellation of both noises (1-4). Various products of ANC have been already introduced in order to improve the interference of the acoustic noise. In this paper, we focus on ANC headrest system and compare the two virtual sensing techniques.

The conventional ANC can get the maximum noise reduction only around error microphones and the size of the Zone of Quite (ZoQ) is limited depending on the target noise's frequency. Moreover, some applications of ANC (e.g. ANC headrest (5-8)) requires that the error microphones have to be located apart from the desired locations (e.g. user's ears) because the error microphones must be installed on the headrest for headrest ANC. To handle the issue, the virtual sensing techniques (5-13) are usually applied to the ANC headrest. In addition, the desired locations (user's ears) may be moved due to user's head movements (it is difficult to fix the head in natural sitting situations). However, if the virtual sensing techniques can work well at every position and in every situation, the ANC headrest can be put into practical use by combining it with physical sensors.

We apply two virtual sensing techniques to the ANC headrest for reducing the broadband noise. One is called Remote Microphone (RM) method; it is valid especially for reducing the narrow band noise (5,6). However, there are two main issues in the RM method. When estimating the transfer function between microphones, some dips often arise at particular frequencies in general acoustic environments. Furthermore, the noise reduction performance strongly depends on the geometric arrangements of primary noise source and error and virtual microphones, that is, the error microphones have to be located closer to the primary noise source than the virtual microphones because the transfer functions from the error microphones to the virtual microphones cannot be obtained if the virtual microphones are closer to the noise source than the error microphones (causality reason). On the other hand, the other method, which is called Auxiliary Filter based Virtual Sensing (AF-VS), is more effective especially for reducing the broadband noise and does not require any geometrical constraint (7-13). In this paper, we compare the two methods on the noise reduction performances for broadband noise to clarify the effectiveness.

The paper is organized as follows. Section 2 explains the limitation of ZoQ and what kind of problems the conventional headrest ANC has. Section 3 introduces the two virtual sensing methods. In Section 4, we show the noise reduction performance of the two method in some situations. Section 5 summarizes the obtained results.

2 LIMITATION OF ZOQ IN THE GENERAL ANC SYSTEM

Zone of Quite (ZoQ) in general ANC systems is formed only around the error microphones. Hence, in the ANC headrest, the ZoQs are created at the back of the headrest. Additionally, the size of ZoQ is 1/10 of the wavelength of the target noise in general ANC systems (2). If the target noise contains high frequency components and the error microphones are located away from desired locations, adequate noise reduction may not be obtained. For instance, when the target noise is 1000 Hz, the ANC system creates the ZoQ whose diameter is 3.4 cm. When one uses the ANC headrest, the positions of the ears may not be located in the ZoQs because people tend to lean forward where the head is not in contact with the headrest. Naturally, the error microphones can not be physically placed close to the user's ears in the ANC headrest. A solution to this limitation of ZoQ is to utilize the virtual sensing techniques. We therefore examine a headrest ANC with virtual sensing techniques in order to validate the effectiveness in various situations.

3 VIRTUAL SENSING TECHNIQUES

3.1 Remote Microphone (RM) Method

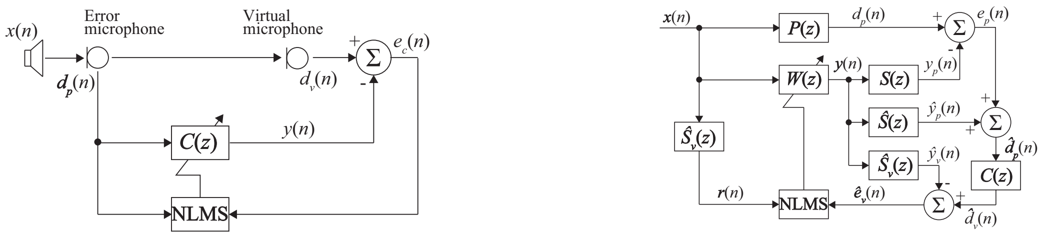

(a) Tuning stage (b) Control stage

Figure 1. Block diagram of feedfoward ANC system with RM.

One way to reduce the target noise at the desired positions is the Remote Microphone (RM) method. The block diagram of the RM method is shown in Fig. 1. In Fig.1, $P(z)$ is the primary path from the reference microphone to the error microphone, $S(z)$ and $S_v(z)$ are the secondary paths from the secondary source to the error and virtual microphones, respectively. In this method, the path from the error microphone to the microphone at the desired position (virtual microphone), $C(z) = V(z) \ / \ P(z)$ is estimated in advance as shown in Fig. 1(a). By using the path, the RM method reduces the target noise at the virtual microphone as shown in Fig. 1(b). However, this method must estimate the path between the microphones which are located a bit far from the noise source. It may cause some dips at some particular frequencies according to the distance, which makes the noise reduction worse. Additionally, depending on the direction of the noise arrival, the causality is not satisfied and $C(z)$ cannot be estimated exactly.

3.2 Auxiliary Filter Based Virtual Sensing (AF-VS) Method

Among virtual sensing techniques, another way is the Auxiliary Filter based Virtual Sensing (AF-VS) method, which is more effective for reducing the broadband noise. The block diagram of the AF-VS method is shown in Fig. 2. As shown in Fig. 2(a), the auxiliary filter $H(z)$ converges $P(z) \ / \ S(z)W_o(z)$. Hence the auxiliary filter includes the information of the optimal noise control filter at the desired position $W_o(z)$. In the control stage, the microphone can not be placed at the desired position and the error signal at the desired position can not be used to update the noise control filter. By using the auxiliary filter $H(z)$ estimated in the tuning stage, this method can reduce the target noise at the desired position. The AF-VS method does not need to estimate the path between the microphones and does not degrade the noise reduction performance unlike the RM method.

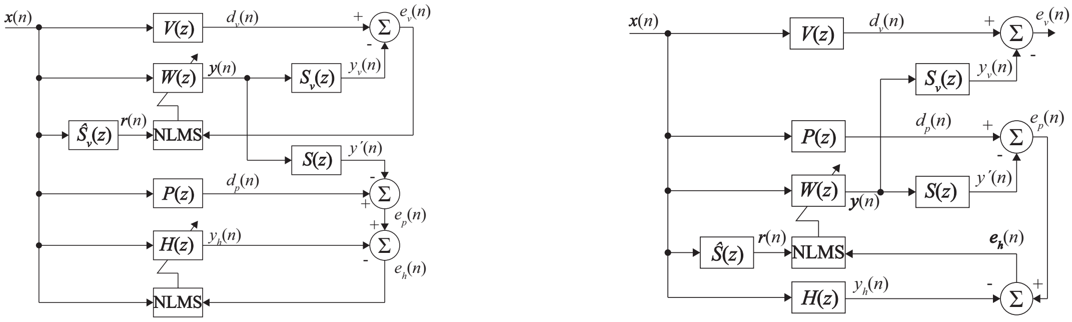

(a) Tuning stage (b) Control stage

Figure 2. Block diagram of single channel feedfoward ANC system with AF-VS.

4 MULTIPLE CHANNEL FEEDFORWARD ANC HEADREST SYSTEM WITH AF-VS

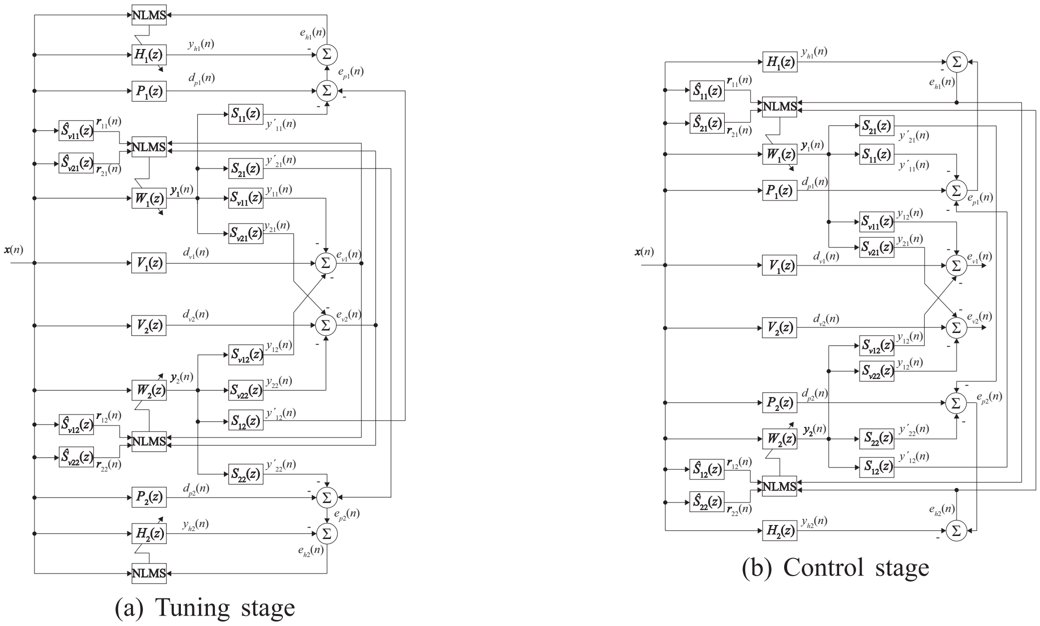

(a) Tuning stage (b) Control stage

Figure 3. Block diagram of multi channel Case (1,2,2) feedfoward ANC system with AF-VS.

In the ANC headrest, there are two secondary sources and two error microphones. When sitting a chair with headrest, the user’s ears are generally apart from the headrest part. In this case, the crosstalk paths (e.g. left secondary source to right error microphone) must be considered in the ANC headrest. In this section, we introduce a multi-channel feedforward ANC headrest system with the AF-VS method. Figure 3 shows block diagrams of the 2 $\times$ 2 adaptive feedforward ANC with the AF-VS method. There are two stages in this method. The first one is called the tuning stage, and the second one is called the control stage. In Fig. 3 (a), the noise control filters and the auxiliary filters on tuning stage are updated by

$$\mathbf{w}_k(n+1) = \mathbf{w}_k(n) + \sum_{m=1}^{2} \frac{\alpha_c}{\beta_c + \|\mathbf{r}_{mk}(n)\|^2} e_{vm}(n)\mathbf{r}_{mk}(n), \tag{1}$$

$$\mathbf{h}_k(n+1) = \mathbf{h}_k(n) + \frac{\alpha_h}{\beta_h + \|\mathbf{x}(n)\|^2} e_{hm}(n)\mathbf{x}(n), \tag{2}$$

$$e_{hm}(n) = e_{pm}(n) - y_{hk}(n), \tag{3}$$

$$r_{mk}(n) = \hat{\mathbf{s}}_{vmk}^T \mathbf{x}(n), \tag{4}$$

where, $k = 1,2$ and $m = 1,2$ express the two secondary sources and the error microphones, respectively. $\mathbf{s}_{mk}$ and $\mathbf{s}_{vmk}$ express the coefficient vectors of the secondary paths from the secondary sources to the error or virtual microphones. $\mathbf{w}_k(n) = [w_{k1}(n), w_{k2}(n), \cdots, w_{kN}(n)]^T$ and $\mathbf{h}_k(n) = [h_{k1}(n), h_{k2}(n), \cdots, h_{kK}(n)]^T$ express the coefficient vectors of the noise control filters W_k and auxiliary filters H_k whose tap lengths are N and K, respectively. $e_{pm}(n)$ and $e_{vm}(n)$ are the error signals at the error and virtual microphones, respectively. $y_{hk}(n)$ expresses the output signals from the auxiliary filter $H_k(z)$ $\hat{\mathbf{s}}_{vmk}$ is the secondary path model of $\mathbf{s}_{vmk}$ and $\mathbf{r}_{mk}(n) = [r_{mk}(n), r_{mk}(n-1), \cdots, r_{mk}(n-N+1)]^T$ is the filtered reference vector in the FXNLMS algorithm. α_c and α_h are the step size parameters of the noise control and the auxiliary, respectively. β_c and β_h are the regularization factors.

In Fig. 3 (b), the error signals at the virtual microphones are given as

$$E_{v1}(z) = \{V_1(z) - S_{v11}(z)W_1(z) - S_{v12}(z)W_2(z)\}X(z), \tag{5}$$

$$E_{v2}(z) = \{V_2(z) - S_{v22}(z)W_2(z) - S_{v21}(z)W_1(z)\}X(z). \tag{6}$$

Hence, the gradients of the noise control filters $W_1(z)$ and $W_2(z)$ are expressed as

$$\frac{\partial E_{v1}^2(z)}{\partial W_1(z)} = 2\{S_{v11}(z)W_1(z) + S_{v12}(z)W_2(z) - V_1(z)\}S_{v11}(z)X^2(z), \tag{7}$$

$$\frac{\partial E_{v1}^2(z)}{\partial W_2(z)} = 2\{S_{v11}(z)W_1(z) + S_{v12}(z)W_2(z) - V_1(z)\}S_{v12}(z)X^2(z), \tag{8}$$

$$\frac{\partial E_{v2}^2(z)}{\partial W_1(z)} = 2\{S_{v21}(z)W_1(z) + S_{v22}(z)W_2(z) - V_2(z)\}S_{v21}(z)X^2(z), \tag{9}$$

$$\frac{\partial E_{v2}^2(z)}{\partial W_2(z)} = 2\{S_{v21}(z)W_1(z) + S_{v22}(z)W_2(z) - V_2(z)\}S_{v22}(z)X^2(z). \tag{10}$$

From (7), (8), (9), and (10), the optimum noise control filters $W_1^o(z)$ and $W_2^o(z)$ given by

$$W_1^o(z) = \frac{S_{v12}V_2(z) - S_{v22}(z)V_1(z)}{S_{v12}S_{v21}(z) - S_{v11}(z)S_{v22}(z)}, \tag{11}$$

$$W_2^o(z) = \frac{S_{v21}V_1(z) - S_{v11}(z)V_2(z)}{S_{v12}S_{v21}(z) - S_{v11}(z)S_{v22}(z)}. \tag{12}$$

Assuming the noise control filters are converged, the error signals for updating the auxiliary filters $H_1(z)$ and $H_2(z)$ are given by

$$\begin{aligned} E_{h1}(z) =& E_{p1}(z) - H_1(z)X(z) \\ =& \{P_1(z) - S_{11}(z)W_1^o(z) - S_{12}(z)W_2^o(z) - H_1(z)\}X(z), \end{aligned} \tag{13}$$

$$\begin{aligned} E_{h2}(z) =& E_{p2}(z) - H_2(z)X(z) \\ =& \{P_2(z) - S_{22}(z)W_2^o(z) - S_{21}(z)W_1^o(z) - H_2(z)\}X(z). \end{aligned} \tag{14}$$

Therefore, $H_1(z)$ and $H_2(z)$ are expressed as

$$\frac{\partial E_{h1}^2(z)}{\partial H_1(z)} = 2\{H_1(z) - P_1(z) + S_{11}(z)W_1^o(z) + S_{12}(z)W_2^o(z)\}X^2(z), \tag{15}$$

$$\frac{\partial E_{h2}^2(z)}{\partial H_2(z)} = 2\{H_2(z) - P_2(z) + S_{22}(z)W_2^o(z) + S_{21}(z)W_1^o(z)\}X^2(z). \tag{16}$$

The optimum auxiliary filters converge to

$$\begin{aligned} H_1^o(z) =& P_1(z) - S_{11}(z)W_1^o(z) - S_{12}(z)W_2^o(z) \\ =& P_1(z) - S_{11}(z)\left\{\frac{S_{v12}V_2(z) - S_{v22}(z)V_1(z)}{S_{v12}S_{v21}(z) - S_{v11}(z)S_{v22}(z)}\right\} - S_{12}(z)\left\{\frac{S_{v21}V_1(z) - S_{v11}(z)V_2(z)}{S_{v12}S_{v21}(z) - S_{v11}(z)S_{v22}(z)}\right\}, \end{aligned} \tag{17}$$

$$\begin{aligned} H_2^o(z) =& P_2(z) - S_{22}(z)W_2^o(z) - S_{21}(z)W_1^o(z) \\ =& P_1(z) - S_{22}(z)\left\{\frac{S_{v21}V_1(z) - S_{v11}(z)V_2(z)}{S_{v12}S_{v21}(z) - S_{v11}(z)S_{v22}(z)}\right\} - S_{21}(z)\left\{\frac{S_{v12}V_2(z) - S_{v22}(z)V_1(z)}{S_{v12}S_{v21}(z) - S_{v11}(z)S_{v22}(z)}\right\}. \end{aligned} \tag{18}$$

We can see that $H_1^o(z)$ and $H_2^o(z)$ in (17) and (18) keep the information of the optimum noise control filters for the virtual microphones including the crosstalk components, respectively.

Whereas, in the tuning stage, the error signals at the virtual microphones can not be used for updating the noise control filters. Instead of (1), the noise control filters in the tuning stage are updated as

$$\mathbf{w}_k(n+1) = \mathbf{w}_k(n) + \sum_{m=1}^{2} \frac{\alpha_c}{\beta_c + \|\mathbf{r}_{mk}(n)\|^2} e_{hm}(n)\mathbf{r}_{mk}(n), \tag{19}$$

$$e_{hm}(n) = e_{pm}(n) - y_{hk}(n), \tag{20}$$

$$r_{mk}(n) = \hat{\mathbf{s}}_{mk}^T \mathbf{x}(n). \tag{21}$$

The error signals for updating the noise control filters are expressed as

$$\begin{aligned} E_{h1}(z) =& E_{p1}(z) - H_1^o(z)X(z) \\ =& P_1(z)X(z) - S_{11}(z)W_1(z)X(z) - S_{12}(z)W_2(z)X(z) - \{P_1(z) - S_{11}(z)W_1^o(z) - S_{12}(z)W_2^o(z)\}X(z), \end{aligned} \tag{22}$$

$$\begin{aligned} E_{h2}(z) =& E_{p2}(z) - H_2^o(z)X(z) \\ =& P_2(z)X(z) - S_{22}(z)W_2(z)X(z) - S_{21}(z)W_1(z)X(z) - \{P_2(z) - S_{22}(z)W_2^o(z) - S_{21}(z)W_1^o(z)\}X(z). \end{aligned} \tag{23}$$

Therefore,

$$\frac{\partial E_{h1}^2(z)}{\partial W_1(z)} = 2[S_{11}(z)\{W_1(z) - W_1^o(z)\} + S_{12}(z)\{W_2(z) - W_2^o(z)\}]S_{11}(z)X^2(z), \tag{24}$$

$$\frac{\partial E_{h1}^2(z)}{\partial W_2(z)} = 2[S_{11}(z)\{W_1(z) - W_1^o(z)\} + S_{12}(z)\{W_2(z) - W_2^o(z)\}]S_{12}(z)X^2(z), \tag{25}$$

$$\frac{\partial E_{h2}^2(z)}{\partial W_1(z)} = 2[S_{21}(z)\{W_1(z) - W_1^o(z)\} + S_{22}(z)\{W_2(z) - W_2^o(z)\}]S_{21}(z)X^2(z), \tag{26}$$

$$\frac{\partial E_{h2}^2(z)}{\partial W_2(z)} = 2[S_{21}(z)\{W_1(z) - W_1^o(z)\} + S_{22}(z)\{W_2(z) - W_2^o(z)\}]S_{22}(z)X^2(z). \tag{27}$$

From (24), (25), (26) and (27), every noise control filter converges to the corresponding optimal ones at the virtual microphones (the desired positions), $W_1^o(z)$ and $W_2^o(z)$ Thus, it can be proved to realize the maximum noise reduction at the desired position without putting the physical microphones there.

5 SIMULATIONS

5.1 Simulation Conditions

In this section, we examine the noise reduction performance at the desired positions (virtual microphones) to compare the effectiveness of the two virtual sensing techniques through some simulations in MATLAB. The measurement arrangements and conditions are shown in Figs. 4, 5 and Table 1.

As shown in Fig. 4, the position of the noise source is located in front of and the back of the ANC headrest in order to investigate the capability for the causality. Moreover, we recorded the noise at the every microphones at the three positions as shown in Fig. 5 in order to examine the robustness for movements of the user's ears (desired positions).

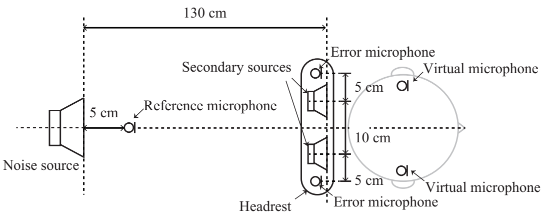

(a) Causality

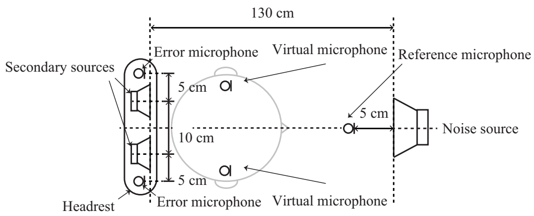

(b) Non-causality

Figure 4. Measurement arrangements.

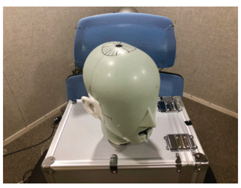
(a) Left


(b) Forward


(c) Right

Figure 5. Three head directions for comparison.

Table 1. Experimental conditions.

Noise	White noise (500 - 2000 Hz)
Update algorithm of filters	NLMS
Tap length of filters W, C and H	500
Step size parameter of filter α	0.05
Regularization parameter β	0.00001
Sampling frequency	12000 Hz
Cut-off frequency of low-pass filter	2500 Hz

5.2 Simulations Results

Due to the limitations of space, the results at the right virtual microphone are shown in this paper. Figure 6 shows the spectra of the error signal at the desired position using the RM and AF-VS methods when the user looks forward like Fig. 5 (b). Next, Fig. 7 illustrates the noise reductions of the two virtual sensing methods in the ANC headrest for three directions of the user's head and two different noise source locations.

As indicated in Fig. 6, the AF-VS can reduce the noise stably between 500 - 2000 Hz regardless of the noise source directions. On the other hand, the RM cannot reduce the target noise especially between 1500 - 2000 Hz and amplifies over 2000 Hz. This is because it is difficult for ANC systems to reduce the high frequency noise. Furthermore, the RM in the non-causality arrangement can reduce the target noise less than on the causality one between 500 - 1500 Hz. This is because $C(z)$ cannot be estimated exactly in the non-causality arrangement.

We summarized the average noise reduction level for three head direction in Table 2. From Fig. 7 and Table 2, the AF-VS gets the almost same noise reduction levels regardless of the noise source position and head directions. On the other hand, the RM amplifies the target noise at the desired position in the non-causality arrangement. Besides, on the causality arrangement, the AF-VS is more effective than the RM for reducing the target noise in the causality arrangement. Additionally, as shown in Fig. 7 (a) and Table 2 (a), the noise reduction performance for the left direction is not very high totally comparing with the other directions because the anti-noise cannot arrive at the desired position directly due to the user's head, which interrupts the path from the secondary source to the desired position.

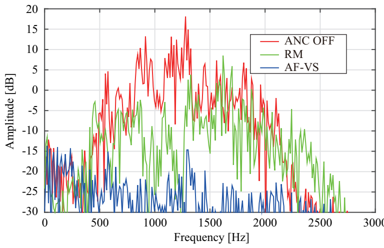

(a) Causality

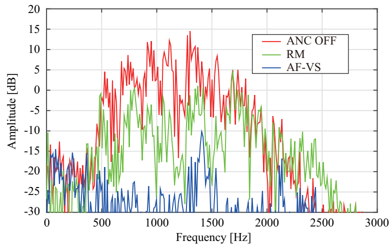

(b) Non-causality

Figure 6. Comparison of error spectra between the two virtual microphone methods.

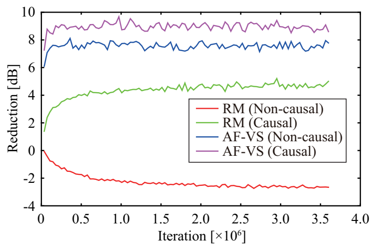

(a) Left

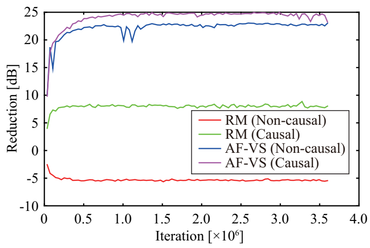

(b) Forward

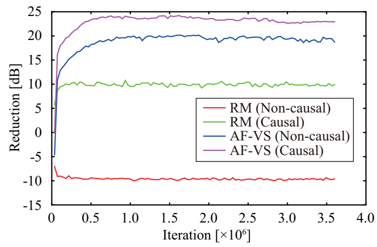

(c) Right

Figure 7. Comparisons of noise reduction between the two virtual microphone methods.

Table 2. Average noise reduction levels for three head directions..

(a) Left

Method Noise source location	RM	AF-VS
Causality	5.00	8.60
Non-causality	-2.65	7.78

(b) Forward

Method Noise source location	RM	AF-VS
Causality	8.03	23.2
Non-causality	-5.44	23.0

(c) Right

Method Noise source location	RM	AF-VS
Causality	9.92	23.9
Non-causality	-9.60	18.7

6 CONCLUSIONS

In order to compare the effectiveness of the two virtual sensing techniques, the RM and AF-VS methods, we adopted the two methods to the ANC headrest. In the simulations, the two methods were compared on the noise reduction performance for broadband noise. As a result, the AF-VS is valid for overall frequency to reduce the target noise regardless of the noise source directions. By contrast, the RM hardly reduces the noise, especially on the non-causality arrangement. Moreover, the AF-VS has higher noise reduction performance than the RM for the three head directions and the two noise source locations.

In the future, we should check whether the ANC headrest system works when the reference microphone is located near the headrest ot chair for the convenience. Moreover, with adding one more secondary loudspeaker and applying Case (1,3,2) or selection type Case (1,2,2), we will try to get the better result for larger space.

REFERENCES

[1] S. M. Kuo and D. R. Morgan, “Active Noise Control: A Tutorial Review,” Proc. of the IEEE, vol. 87, no. 6, pp. 943–973, Jun. 1999.

[2] S. J. Elliott, Signal Processing for Active Control, Academic Press, San Diego, CA, 2001.

[3] Y. Kajikawa, W. S. Gan and S. M. Kuo, “Recent Advances on Active Noise Control: Open Issues and Innovative Applications,” APSIPA Transactions on Signal and Information Processing, vol. 1, Aug. 2012.

[4] P. Lueg, “Process of Silencing Sound Oscillations,” U. S. patent 2043416, Jun. 1936.

[5] D. Moreau, B. Cazzolato, A. Zander and C. Petersen, “A Review of Virtual Sensing Algorithms for Active Noise Control,” *Algorithms.*, vol. 1, no. 2, pp. 69–99, Nov. 2008.

[6] D. P. Das, D. J. Moreau, B. S. Cazzolato, “Performance Evaluation of an Active Headrest Using the Remote Microphone Technique,” Acoustics 2011, pp. 1–7, Gold Coast, Australia, Nov. 2011

[7] J. Garcia-Bonito, S. J. Elliott, C.C. Boucher, “Generation of Zones of Quiet Using a Virtual Microphone Arrangement“ The Journal of the Acoustical Society of America, vol. 101, issue 6, pp. 34983516, 1997.

[8] S. J. Elliott, M. Simon-Galvez, J. Cheer, W. Jung, “Head Tracking for Local Active Sound Control“ In 12th Western Pacific Acoustics Conference 2015, pp. 385389, Singapore, 2015.

[9] R. Hasegawa, Y. Kajikawa, C. Chang and S. Kou “Headrest Application of Multi-Channel Feedback Active Noise Control with Virtual Sensing," in Internoise 2017, Hong Kong, Aug. 2017.

[10] S. Hirose and Y. Kajikawa “Effectiveness of Headrest ANC System with Virtual Sensing Technique for Factory Noise," in APSIPA Transactions on Signal and Information Processing, Malaysia, Dec. 2018.

[11] N. Miyazaki, and Y. Kajikawa, “Head-Mounted Active Noise Control System with Virtual Sensing Technique,” *J. Sound Vib.*, vol. 339, pp. 65–83, Mar. 2015.

[12] S. Edamoto, C. Shi, and Y. Kajikawa, “Virtual Sensing Technique for Feedforward Active Noise Control," in *Proc. the 5th Joint Meeting ASA. and ASJ.*, Honolulu, USA, Nov. 2016.

[13] R. Maeda, Y. Kajikawa, C.-Y. Chang, S. M. Kuo, “Active Noise Control for Motor Bike Helmet Using Virtual Sensing, 25th International Congress on Sound and Vibrations, Hiroshima, Japan, Jul. 2018.